

Consistent Pose Uncertainty Estimation for Spherical Cameras

Bernd Krolla
DFKI - German
Research Center for
Artificial Intelligence
bernd.krolla@dfki.de

Christiano Couto Gava
DFKI - German
Research Center for
Artificial Intelligence
christiano.gava@dfki.de

Alain Pagani
DFKI - German
Research Center for
Artificial Intelligence
alain.pagani@dfki.de

Didier Stricker
DFKI - German
Research Center for
Artificial Intelligence
didier.stricker@dfki.de

ABSTRACT

In this work, we discuss and evaluate the reliability of first order uncertainty propagation results in context of spherical *Structure from Motion*, concluding that they are not valid without restrictions, but depend on the choice of the objective function. We furthermore show that the choice of the widely used geodesic error as objective function for a reprojection error optimization leads to disproportional pose uncertainty results of spherical cameras.

This work identifies and outlines alternative objective functions to bypass those obstacles by deducing Jacobian matrices according to the chosen objective functions with subsequent conduction of first order uncertainty propagation. We evaluate the performance of the different objective functions in different optimization scenarios and show that best results for uncertainty propagation are obtained using the Euclidean distance to measure deviations of image points on the spherical image.

Keywords

Computer vision, 3D reconstruction, spherical imaging, uncertainty propagation, error propagation, camera pose optimization, spherical SfM

1 INTRODUCTION

Spherical imaging recently experienced increasing attention, since projects such as Microsoft's *StreetSide* or Google's *Street View* [3] provide numerous spherical images to online users. Furthermore, imaging devices for professional [35, 41] or private consumers [8, 17] widen the user groups being able to capture spherical images.

The availability of multiple spherical images of a scene allows for its reconstruction based on spherical Structure from Motion (SfM). But while spherical SfM is well understood [31, 39], *uncertainty propagation* throughout the applied algorithms is often neglected.

Though the consideration of input parameter uncertainties and their propagation allows for a confidence quantification of obtained results and can be utilized for outlier rejection, accuracy estimation of the reconstruction or mesh generation. The current work therefore proposes the consistent estimation of camera pose uncer-

tainties for spherical cameras by applying uncertainty propagation steps through spherical SfM algorithms.

In this context, the applied mathematical optimization steps represent an essential component, which is in general for science and in particular for computer vision a wide spread approach to retrieve optimal solutions for mathematical problem statements. Especially over-parametrized systems of equations in combination with noisy input parameters do commonly not allow for analytically exact solutions. Therefore, a huge variety of prominent optimization algorithms such as Gauss-Newton or Levenberg-Marquardt [24] is available to handle such problem formulations by identifying globally optimal solutions.

These algorithms essentially rely on the formulation of objective functions to rate the quality of estimated solutions. The derivation or numerical approximation of Jacobian matrices from these functions with respect to the input parameters in the course of the optimization process is necessary to determine the direction of further convergence towards an optimal solution (Figure 1).

When performing first order uncertainty propagation, such an optimal solution is chosen as linearization point to derive the Jacobian matrix of the objective function with respect to the provided input parameters. This allows a reliability quantification of the resulting solution based on uncertainties of the input parameters.

Permission to make digital or hard copies of all or part of this work for personal or classroom use is granted without fee provided that copies are not made or distributed for profit or commercial advantage and that copies bear this notice and the full citation on the first page. To copy otherwise, or republish, to post on servers or to redistribute to lists, requires prior specific permission and/or a fee.

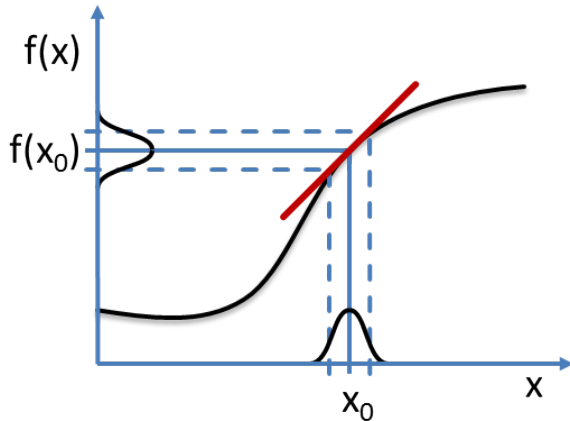


Figure 1: Outline of first order uncertainty propagation: Assuming x_0 to identify a position of interest for a given measurement function, the first derivative of $f(x)$ at x_0 (red/thick line) is calculated to quantify the resulting uncertainty for $f(x_0)$ from the uncertainty of parameter x . For a m -dimensional function $f(\mathbf{x})$, depending from n parameter $\mathbf{x} = (x_1, x_2, \dots, x_n)$, the derivatives with respect to the elements of \mathbf{x} are commonly summarized in a $m \times n$ Jacobian matrix.

Related work: Applying the Monte Carlo method [25] is a very general and resource intensive way to perform uncertainty propagation. The algorithm of interest is executed multiple times with varying input parameters and the influence of individual input parameters onto the result can be deduced. Since the number of required iterations scales highly nonlinear with the number of input parameters this method was not considered in the current work.

Applying the concept of unscented transform [18] allows for a less resource intensive deduction of uncertainties for a given algorithm by choosing representative *sigma points*. The distribution of sigma points within the domain of input parameters is known. Evaluating their distribution within the results domain allows then for the deduction of resulting uncertainties from input uncertainties.

Within the current work, we considered first order uncertainty propagation, since the requirement of linearization around the optimal point yields acceptable results. When focusing on the topic of SfM, various contributions recently considered different parts of the reconstruction pipeline under the aspects of uncertainty propagation:

To give a measure for the location uncertainty of extracted image features from a given set of input images, Zeisl et al. provided an estimation of location uncertainty for scale invariant feature points [44] with evaluations for SIFT [23] and SURF [4] features. When it comes to the subsequent feature matching process

within images, the work of Ochoa and Belongie [29] discusses the propagation of uncertainties for guided matching techniques.

Sur et al. introduced approaches to perform uncertainty propagation through the 8-point algorithm, which is needed to calibrate initial camera poses against each others [37, 38]. Di Leo et al. introduced a method for covariance propagation to estimate uncertainties in stereo vision [9], whereas Eudes et al. provide an approach for error propagation for local bundle adjustment [11]. Apart from the SfM reconstruction focus, Bleser et al. introduced in their work methods for error propagation through SLAM-algorithms [5].

Outline: The proposed approach is outlined in Section 2. Evaluation and results are elaborated in Section 3. Section 4 concludes this work.

2 METHOD

In the course of this work, the considered uncertainties are assumed to be Gaussian-distributed, so that their propagation is achieved by propagating their corresponding 1- σ -environment represented by a covariance matrix. For a given function $f: x \mapsto y$ with $x \in \mathbb{R}^n$, $y \in \mathbb{R}^m$ a linear uncertainty propagation is obtained as [16]

$$\text{cov}(y) = \left(\frac{\partial f}{\partial x} \right) \text{cov}(x) \left(\frac{\partial f}{\partial x} \right)^T \quad (1)$$

The calculation of Jacobian matrices $\frac{\partial f}{\partial x}$ corresponds to the first term of a Taylor expansion and approximates the original function linearly, while relying on the differentiability of the objective function at the point of the resulting solution.

Examining the pose uncertainty estimation of spherical cameras, we elaborate in this work the consequences of non-differentiability at the point of an optimal solution. For this purpose a scenario of uncertainty propagation will be considered, which quantifies camera pose uncertainties of spherical cameras from uncertainties of extracted image features. To study and avoid non-differentiabilities, different objective functions for pose optimization will be introduced and evaluated. But prior to outlining the detailed problem statement, we introduce needed definitions as well as the underlying concept of Structure from Motion (SfM), which was considered for this work.

Specific background: We consider as input data for the optimization problem a set of unordered images with overlapping field of view (FOV) from a given scene, such as [34, 36] or datasets on [1]. To make use of such a set of images, many processing approaches in the field of computer vision rely on the recovery of the camera parameters [10, 13, 19, 28]. The minimal set of camera

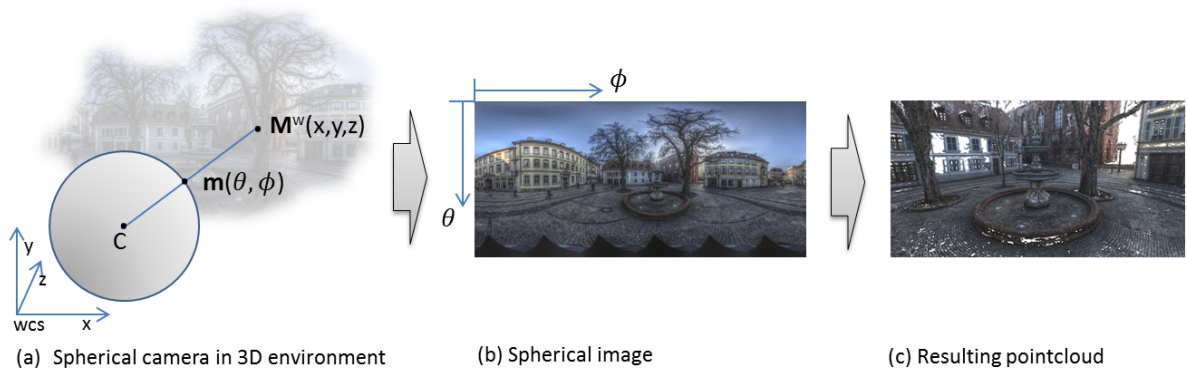


Figure 2: (a) Projection of a 3D point $\mathbf{M}^w(x,y,z)$ in world coordinate system wcs to its image point $\mathbf{M}^s(\theta, \phi)$ (short: \mathbf{m}) for a spherical camera on position \mathbf{C} . (b) The resulting image of the camera, used in the course of this work, is a high dynamic range (HDR) image with a resolution of $7'000 \times 14'000$ pixel. The images are parametrized in the image coordinate system (ics) using spherical coordinates $\theta[0, \pi]$ and $\phi[0, 2\pi]$. (c) Out of these images, a 3D pointcloud representing the captured environment is finally obtained.

parameters to be recovered consists of extrinsic parameters specifying the transformation (translation \mathbf{t}^{cw} and rotation \mathbf{R}^{cw}) from the world coordinate system (wcs) into the camera coordinate system (ccs).

This set of parameters is commonly accompanied by a set of intrinsic parameters, depending on the used camera type. For perspective cameras, they list up to focal length in relation to CCD-chip-size, principal point as well as skew-value and are commonly considered in the camera matrix \mathbf{K} [14]. Existing radial or tangential lens distortion as described in [15] can be summarized to a distortion function \mathbf{D} . \mathbf{K} and \mathbf{D} can be recovered from the images of the scene [6, 26, 32], from accompanied exif-data or from previously taken images depicting special calibration patterns [7, 40]. Since for the present work, a spherical camera was used [41], no intrinsic but only extrinsic parameters have to be recovered [31]. The resulting spherical images are hereby considered as a mapping from a given three-dimensional environment through the camera center onto a unit sphere, making the definition of intrinsic parameter obsolete (Figure 2).

To regain the needed extrinsic camera parameters in this work, image feature extraction and matching was performed. To account for the spherical character of the images, a modified version of affine SIFT features (A-SIFT) [23, 27] was applied to extract in average up to 100'000 features per image. The process of feature matching was hereby constraint by the simultaneous estimation of the *Essential Matrix* as proposed by Laganière [21], resulting in a significantly more accurate set of feature matches between image pairs.

The subsequent camera calibration to regain the extrinsic parameters is split into the following two steps:

Firstly a rough guess of camera positions was estimated for two images. This linear alignment step uses the essential matrix \mathbf{E} estimated from matched image features [14] to align two initial cameras against each other. Further camera positions were then estimated through alignment towards the triangulated 3D points of the first two cameras by applying the concept of 2D-3D correspondences. These correspondences were used to solve the PnP-problem by exploiting the *EPnP*-algorithm as proposed by Moreno-Noguer et al. [12].

In a second step, the obtained rough alignment of camera poses and 3D points is optimized by applying non-linear optimization techniques. To perform this task a wide range of implementations such as [2, 22, 42, 43] is at hand. The authors of this work chose the implementation of Lourakis et al. [22], which uses internally the Levenberg-Marquardt optimization.

To formulate/provide the required measurement function the *collinearity constraint* described by Schenk [33] was applied. This constraint assumes 3D points \mathbf{M}^w , the cameras center of projection \mathbf{C} and the image point \mathbf{M}^s (short: \mathbf{m}) to be in line. A general formulation, which holds for perspective and spherical cameras enforces the cross product between the according vectors to be zero:

$$\mathbf{m} \times (\mathbf{R}^{cw} \cdot \mathbf{M}^w + \mathbf{t}^{cw}) = \mathbf{m} \times \mathbf{M}^c \stackrel{!}{=} 0 \quad (2)$$

with \mathbf{M}^w representing a 3D point in wcs , \mathbf{M}^c describing this point in ccs and \mathbf{m} its corresponding image point within the spherical image coordinate system ($sics$).

Deviations from this constraint during the registration process are mainly caused by non-optimized model parameter (camera parameter + 3D points) and are de-

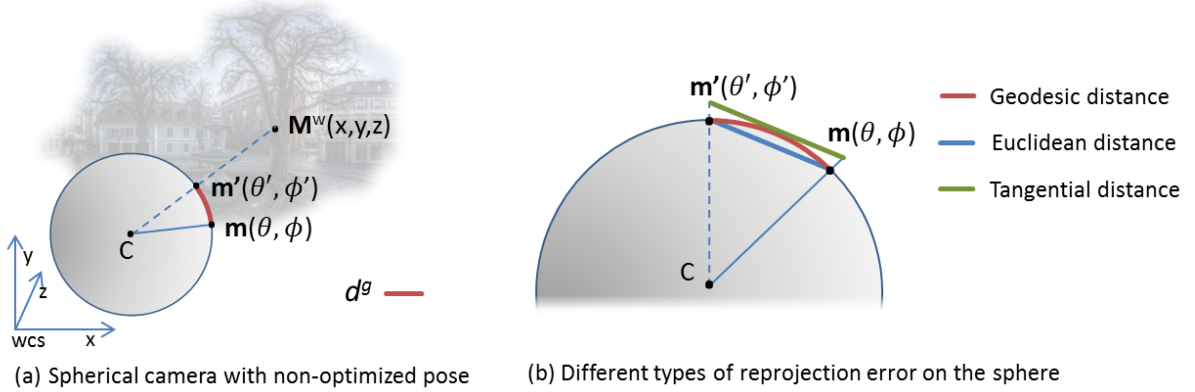


Figure 3: (a) The geodesic distance d^g between an image point \mathbf{m} and the corresponding backprojection on a unit sphere \mathbf{m}' as defined in Equation 4. The collinearity constraint for cameras assumes 3D points, the center of projection and the projection of the 3D points onto the image sensor to be in line. (b) Deviations from this constraint are quantified as reprojection error.

scribed by the concept of *reprojection error* d (Figure 3). Averaging this error d between image point \mathbf{m} and the reprojection \mathbf{m}' of the corresponding 3D point \mathbf{M}^w for all k 3D points leads to the averaged reprojection error \bar{d} and allows a rating of the overall optimization quality:

$$\bar{d} = \frac{1}{k} \sum_{j=1}^k d(\mathbf{m}^j, \mathbf{m}'^j) \quad (3)$$

Since differently formulated objective functions can be applied to perform the optimization step outlined above, the introduced distance d has to be computed in a corresponding manner. Examples are the *squared distance* in case of perspective images or, for the considered spherical scenario, error models such as *geodesic error*, *projected distance*, *tangential error for epipolar distance* or *tangential error for reprojection distance* as proposed by Pagani et al. [31].

The mentioned objective functions approximate the exact formulation of the geodesic distance d^g for a given 2D-3D correspondence

$$d^g(\mathbf{m}^T \mathbf{m}') = \cos^{-1}(\mathbf{m}^T \mathbf{m}') \quad (4)$$

for spherical images and represent valid approaches to perform global optimization with varying quality of the results as detailed in [31].

We demonstrate below, that such an approximation of Equation 4 is even necessary to perform first order uncertainty propagation, since the geodesic distance d^g results in corrupt uncertainty estimations as shown below.

Problem statement: When minimizing the geodesic distance d^g between two points \mathbf{m} and \mathbf{m}' , the scalar

product $(\mathbf{m}^T \mathbf{m}')$ converges to 1. For the first order derivative of d^g , we obtain then

$$d'^g = \frac{d d^g(\mathbf{m}^T \mathbf{m}')}{d(\mathbf{m}^T \mathbf{m}')} = -\frac{1}{\sqrt{1 - (\mathbf{m}^T \mathbf{m}')^2}} \quad (5)$$

which encloses a singularity for $(\mathbf{m}^T \mathbf{m}') = 1$ (Figure 4b). For $(\mathbf{m}^T \mathbf{m}') \rightarrow 1$, we furthermore obtain

$$\lim_{(\mathbf{m}^T \mathbf{m}') \rightarrow 1} \frac{d d^g(\mathbf{m}^T \mathbf{m}')}{d(\mathbf{m}^T \mathbf{m}')} = -\infty, \quad (6)$$

implying that good optimization results ($(\mathbf{m}^T \mathbf{m}') \approx 1$) exclude a meaningful first order uncertainty propagation: When relying on the geodesic distance d^g as the measurement function, improvements of the camera pose estimation at constant input parameters will result in an increased pose uncertainty.

2.1 Approach

As previously motivated, the geodesic distance function d^g (Equation 4) is not suitable for consistent first order uncertainty propagation.

Therefore we evaluate multiple approximations of d^g such as the tangential distance d^t with

$$d^t = 2\sqrt{\frac{1 - \mathbf{m} \cdot \mathbf{m}'}{1 + \mathbf{m} \cdot \mathbf{m}'}} \quad (7)$$

as well as the Euclidean distance d^e between \mathbf{m} and \mathbf{m}' to perform camera pose optimization and first order uncertainty propagation within the context of spherical imaging. d^e is hereby given as

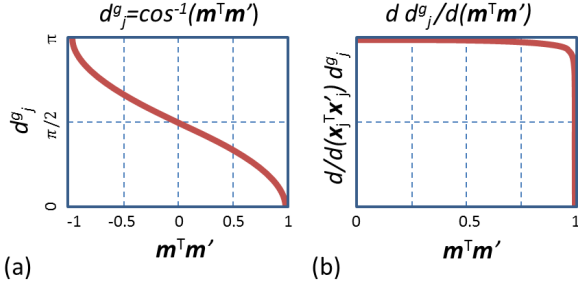


Figure 4: (a) Error measure d^g given as scalar product between \mathbf{m} and \mathbf{m}' with optimized result at $(\mathbf{m}^T \mathbf{m}') = 1$. (b) The first derivative of d^g shows the infinite descend of the geodesic distance d^g when \mathbf{m} and \mathbf{m}' are aligned parallel against each other ($(\mathbf{m}^T \mathbf{m}') \rightarrow 1$). When performing first order uncertainty propagation leads this to infinite impact of an arbitrarily small error (See Figure 1).

$$d^e = \|\mathbf{m} - \mathbf{m}'\| \quad (8)$$

as shown in Figure 3.

Camera pose optimization was therefore done by minimizing the Euclidean distance d^e between the unit vectors \mathbf{m} and \mathbf{m}' . To constrain all vectors \mathbf{m} and \mathbf{m}' throughout the optimization to unit length, a normalization of the vectors was considered.

Since, in contrast to d^g , the first order derivative of d^e is bounded and non-singular for $(\mathbf{m}^T \mathbf{m}') \approx 1$, a consistent estimation of the resulting camera pose uncertainty can be deduced as outlined in the following:

Considering \mathbf{m}' as reprojection of the 3D point \mathbf{M}^c corresponding to \mathbf{m} , we can reformulate d^e as

$$\begin{aligned} d^e &= \|\mathbf{m} - \mathbf{m}'\| = \left\| \mathbf{m} - \frac{\mathbf{M}^c}{\|\mathbf{M}^c\|} \right\| \\ &= \left\| \mathbf{m} - \frac{\mathbf{R}^{cw} \mathbf{M}^w + \mathbf{t}^{cw}}{\|\mathbf{R}^{cw} \mathbf{M}^w + \mathbf{t}^{cw}\|} \right\|. \end{aligned} \quad (9)$$

Derivation of Jacobians: To perform first order uncertainty propagation with the proposed Euclidean measurement function (Equation 8), the according Jacobian matrices were derived towards all input parameters based on the rewritten Equation 9. The indices $j, k, l \in \{1, 2, 3\}$ identify thereby the components of the respective vectors. For the different Jacobian matrices, we obtain:

- Jacobian towards \mathbf{m} :

$$\frac{\partial d_j^e}{\partial \mathbf{m}_k} = \delta_{jk} \quad (10)$$

with δ_{jk} as Kronecker delta

$$\delta_{jk} = \begin{cases} 1 & j = k \\ 0 & j \neq k \end{cases} \quad (11)$$

- Jacobian towards \mathbf{M}^w :

$$\frac{\partial h_j}{\partial \mathbf{M}_k^w} = \mathbf{M}_j^c \left(\sum_{l=1}^3 \mathbf{R}_{lk}^{cw} \mathbf{M}_l^c \right) - \frac{\mathbf{R}_{jk}^{cw}}{\|\mathbf{M}^c\|} \quad (12)$$

- Jacobian towards \mathbf{R}^{cw} :

$$\frac{\partial h_j}{\partial \mathbf{R}_{kl}^{cw}} = -\frac{1}{\chi} \mathbf{M}_j^c \mathbf{M}_k^c \mathbf{M}_l^w - \delta_{jk} \frac{\mathbf{M}_l^w}{\|\mathbf{M}^c\|} \quad (13)$$

with

$$\chi = ((\mathbf{M}_x^c)^2 + (\mathbf{M}_y^c)^2 + (\mathbf{M}_z^c)^2)^{3/2} \quad (14)$$

- Jacobian towards \mathbf{t}^{cw} :

$$\frac{\partial h_j}{\partial \mathbf{t}_k^{cw}} = -\frac{1}{\chi} \mathbf{M}_j^c \mathbf{M}_k^c - \delta_{jk} \frac{1}{\|\mathbf{M}^c\|} \quad (15)$$

Relying on those derivations, the final expression for the impact of the uncertainty σ_n of spherical image points represented through the normal vector representation proposed in [20] onto the camera pose uncertainty σ_{cp} sums up to:

$$\sigma_{cp} = \left(\left(\frac{\partial h_j}{\partial \mathbf{t}_k^{cw}} \right)^T \cdot \xi^{-1} \cdot \left(\frac{\partial h_j}{\partial \mathbf{t}_k^{cw}} \right) \right)^{-1} \quad (16)$$

with

$$\xi = \left(\frac{\partial h_j}{\partial \mathbf{M}_k^w} \right) \sigma_{3D_w} \left(\frac{\partial h_j}{\partial \mathbf{M}_k^w} \right)^T + \left(\frac{\partial d_j^e}{\partial \mathbf{m}_k} \right) \sigma_n \left(\frac{\partial d_j^e}{\partial \mathbf{m}_k} \right)^T \quad (17)$$

Analogously, we deduced the corresponding Jacobian matrices for d^l and d^g as error measure, being evaluated in the following section.

3 EVALUATION AND RESULTS

We evaluated the impact of the different error measures onto the resulting pose uncertainty estimation of the spherical cameras. The considered image points of the spherical images were hereby extracted from images of the St.-Martinsplatz dataset (Figure 2(b)) with a resolution of 14000×7000 pixel [30]. Since those images provide easily up to 100000 features when applying feature extraction algorithms, only a small subset of features of the original number of features was used. This allowed for a reasonable resource consumption using Matlab software, whereas especially the inversion of the matrices as introduced in Equation 16 implied maximum processing load throughout the runtime of the algorithm. In the course of this evaluation further assumptions were introduced, diverging from the standard processing approaches to obtain 3D reconstruction

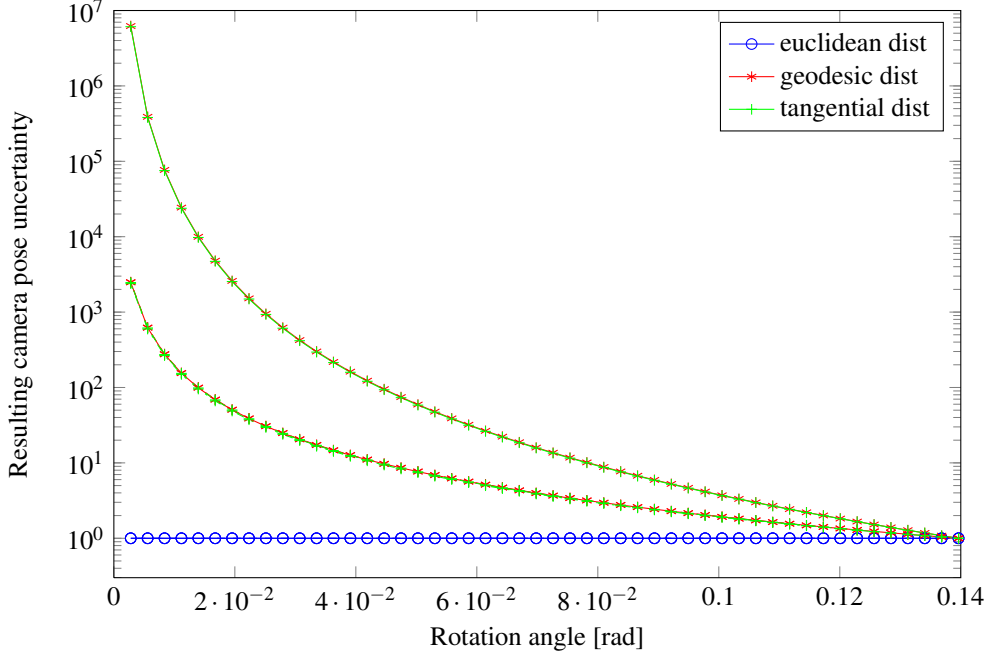


Figure 5: Deduced Jacobians for different measurement functions (d^e , d^g , d^t) influence the pose uncertainty estimation within the directed reprojection error scenario. When approaching the optimal camera pose by minimizing the appropriate reprojection error towards 0 (Right to left on the x-axis), only the Euclidean distance d^e allows for a deduction of constant Jacobians, which is a necessary precondition to perform consistent camera pose uncertainty estimation, by depending on the uncertainties of the input data and not on the degree of pose optimization. Within the figure, the size of the three uncertainty ellipsoid components of the camera pose are plotted for each measurement function (—, - -, - ·, partially overlapping), being normalized against their initial value. Within this scenario, the rotation axis was set to $\mathbf{r}_\alpha = (1, 1, 1)^T$ (see Section 3). Note furthermore the logarithmic scaling of the ordinate.

results but allowing for an evaluation of additional aspects of the uncertainty estimation of the camera pose. To enhance the comparability of the impact of feature uncertainties, they were initialized with identical values, while for uncertainty propagation within standard 3D reconstruction pipelines methods such as [44] are more appropriate, since the individual location uncertainties of feature points based on gradient analysis is assured.

Reprojection errors between the previously extracted 2D image feature points and the back projected 3D points were furthermore parametrized for the evaluation process, in order to control a simulated optimization process (= *minimization of reprojection errors*) properly. Afterwards, a successive optimization of the camera pose was simulated by iteratively minimizing the reprojection error of the 3D points towards the 2D image point.

The effect of the different measurement functions was evaluated with respect to the pose uncertainty of the spherical camera under two different aspects:

Directed reprojection error evaluation: After back projecting the 3D points onto the sphere to obtain the image points, the camera was rotated by a predefined

angle α around an axis \mathbf{r}_α . This rotation angle α along the axis \mathbf{r}_α (here: $\mathbf{r}_\alpha = (1, 1, 1)^T$) was reduced iteratively through the evaluation process to simulate an optimization of the camera pose.

The obtained results are shown in Figure 5. Note that the rotation angle along \mathbf{r}_α was reduced iteratively from 0.14rad towards 0rad (reading the diagram from *right to left*). Since the covariances of the input variables – namely the uncertainty regions of the image features – remained constant throughout the optimization process, a constant camera pose uncertainty is expected as output. Considering the differently deduced Jacobian matrices, this constant camera pose uncertainty is only assured for the objective function based on the Euclidean distance d^e as introduced above.

Undirected reprojection error evaluation: In a second evaluation scenario, a set of randomly generated 3D points was back projected onto the sphere to obtain 2D image points. Afterwards, Gaussian-distributed noise was added to the 3D points and they were once again reprojected onto the sphere. This noise was iteratively reduced to simulate an optimization of the camera pose. Deviating from the *directed reprojection error evaluation*, where all deviations between image points

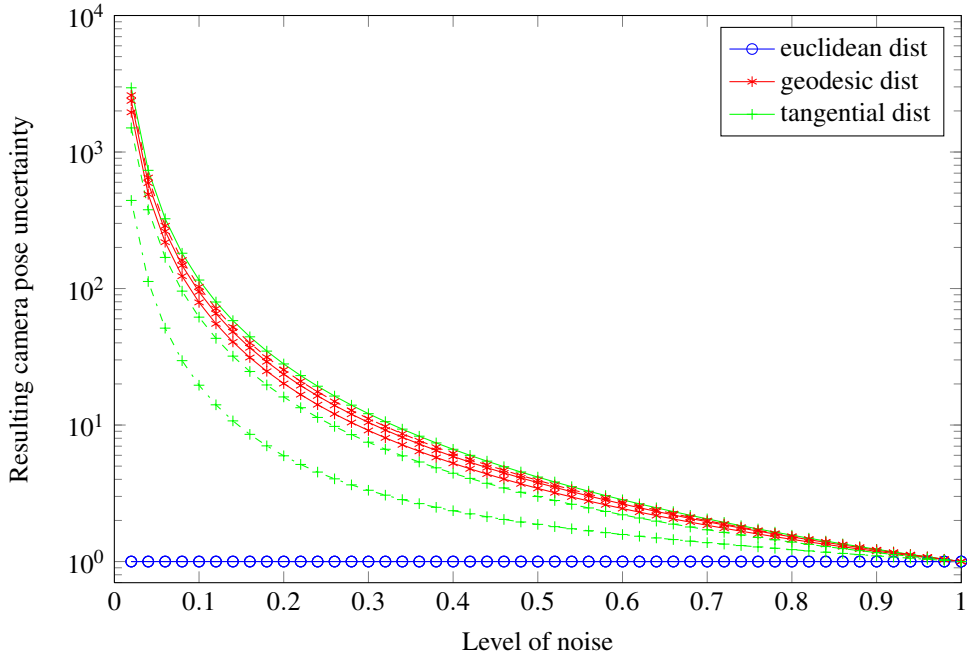


Figure 6: Visualization of the impact of deduced Jacobians for different measurement functions (d^e , d^g , d^t) for the undirected reprojection error scenario. When approaching the optimal camera pose by minimizing the appropriate reprojection error towards 0 (Right to left on the x-axis), also within this scenario allows exclusively the Euclidean distance d^e for a deduction of constant Jacobians. This is a necessary precondition to perform consistent camera pose uncertainty estimation, by depending on the uncertainties of the input data and not on the degree of pose optimization. Within the figure, the size of the three uncertainty ellipsoid components of the camera pose is plotted for each measurement function (—, --, - · -, partially overlapping), being normalized against their initial value. Note furthermore the logarithmic scaling of the ordinate.

\mathbf{m} and back projected 3D points \mathbf{m}' had one common predominant direction, the reprojection errors within this scenario are distributed unconstrained in all directions, leading to random noise-like deviations.

But also in this evaluation scenario entails a reduction of the noise-level, which corresponds to a continuous approximation towards an optimized solution, a constant change of the involved Jacobian matrices for almost all error measures. As in the first scenario leads this to a continuously varying pose uncertainty estimation, which is not scaling with the actual expectations of constant uncertainty estimation.

Exclusively, the evaluated Euclidean distance d^e between 2D image points \mathbf{m} and reprojected 3D points \mathbf{m}' leads as expected to constant Jacobians allowing for a consistent pose uncertainty estimation of spherical cameras throughout the optimization process.

4 CONCLUSION

In the course of this work, we evaluated different objective functions to perform reasonable uncertainty propagation in SfM-frameworks using spherical images. On the basis of those differently designed functions the uncertainty estimation of spherical camera poses was evaluated throughout different optimization scenarios.

Relying on the gained insights, we conclude, that a reliable and consistent uncertainty estimation can not be performed on arbitrarily designed objective functions, since in general the deduced Jacobians tend to concede disproportionately high impact to small errors, when it comes to an iterative optimization of spherical camera poses. Basing on our evaluations, we suggest the evaluated Euclidean distance d^e to perform uncertainty propagation in a consistent manner, since this function exclusively assures constant result for Jacobian matrices as elaborated in this work.

Within the presented work, we deduced Jacobian matrices for the examined objective functions and evaluated the resulting camera pose optimization results. In general, is it worth to mention that especially the inversion of the deduced Jacobian matrices, as outlined throughout this work, represents a significant obstacle in terms of high processing costs, which has to be tackled whenever numerous points are considered.

ACKNOWLEDGEMENTS

This work was funded by the BMBF-projects CAPTURE (01IW09001) and DENSITY (01IW12001).

REFERENCES

- [1] <http://www.flickr.com/>, 2014.
- [2] Sameer Agarwal and Keir Mierle. Ceres solver. <https://code.google.com/p/ceres-solver/>, 2012.
- [3] D. Anguelov, C. Dulong, D. Filip, C. Frueh, S. Lafon, R. Lyon, A. Ogale, L. Vincent, and J. Weaver. Google street view: capturing the world at street level. *IEEE Computer*, 43(6):32–38, 2010.
- [4] Herbert Bay, Tinne Tuytelaars, and Luc Van Gool. Surf: Speeded up robust features. *ECCV*, 2006.
- [5] Gabriele Bleser, Mario Becker, and Didier Stricker. Real-time vision-based tracking and reconstruction. *Journal of Real-Time Image Processing*, 2:161–175, 2007.
- [6] Sylvain Bougnoux. From projective to euclidean space under any practical situation, a criticism of self-calibration. In *Computer Vision, 1998. Sixth International Conference on*, pages 790–796. IEEE, 1998.
- [7] Jean-Yves Bouguet. Camera calibration toolbox for matlab, http://www.vision.caltech.edu/bouguetj/calib_doc/, 2010.
- [8] Ricoh Company. Ricoh theta <http://theta360.com/en/>, 2013.
- [9] G. Di Leo, C. Liguori, and A. Paolillo. Covariance propagation for the uncertainty estimation in stereo vision. *Instrumentation and Measurement, IEEE Transactions on*, 60(5):1664–1673, 2011.
- [10] Hugh Durrant-Whyte and Tim Bailey. Simultaneous localization and mapping: part i. *Robotics & Automation Magazine, IEEE*, 13(2):99–110, 2006.
- [11] A. Eudes and M. Lhuillier. Error propagations for local bundle adjustment. In *Computer Vision and Pattern Recognition, 2009. CVPR 2009. IEEE Conference on*, pages 2411–2418, june 2009.
- [12] F. Moreno-Noguer, V. Lepetit, and P. Fua. Accurate non-iterative o(n) solution to the pnp problem. In *IEEE International Conference on Computer Vision*, Rio de Janeiro, Brazil, October 2007.
- [13] Yasutaka Furukawa and Jean Ponce. Accurate, dense, and robust multiview stereopsis. *IEEE Transactions on Pattern Analysis and Machine Intelligence*, 32:1362–1376, 2010.
- [14] R. I. Hartley and A. Zisserman. *Multiple View Geometry in Computer Vision*. Cambridge University Press, 2000.
- [15] Janne Heikkila and Olli Silven. A four-step camera calibration procedure with implicit image correction. In *Computer Vision and Pattern Recognition, 1997. Proceedings., 1997 IEEE Computer Society Conference on*, pages 1106–1112. IEEE, 1997.
- [16] Gustaf Hendeby. *Performance and Implementation Aspects of Nonlinear Filtering*. PhD thesis, Linköping University, 2008.
- [17] Tamaggo Inc. Tamaggo 360-imager - <http://www.tamaggo.com/>.
- [18] Simon J Julier and Jeffrey K Uhlmann. Unscented filtering and nonlinear estimation. *Proceedings of the IEEE*, 92(3):401–422, 2004.
- [19] Georg Klein and David Murray. Parallel tracking and mapping for small AR workspaces. In *Proc. Sixth IEEE and ACM International Symposium on Mixed and Augmented Reality (ISMAR'07)*, Nara, Japan, November 2007.
- [20] B. Krolla, G. Bleser, Y. Cui, and D. Stricker. Representing feature location uncertainties in spherical images. *International Conference in Central Europe on Computer Graphics, Visualization and Computer Vision, WSCG*, 2013.
- [21] Robert Laganière. *OpenCV 2 computer vision application programming cookbook*. Packt Publishing, 2011.
- [22] M.I. A. Lourakis and A.A. Argyros. Sba: A software package for generic sparse bundle adjustment. *ACM Trans. Math. Software*, 36(1):1–30, 2009.
- [23] D.G. Lowe. Distinctive image features from scale-invariant keypoints. *International Journal of Computer Vision*, 60(2):91–110, 2004.
- [24] Donald W Marquardt. An algorithm for least-squares estimation of nonlinear parameters. *Journal of the Society for Industrial & Applied Mathematics*, 11(2):431–441, 1963.
- [25] Daniel D McCracken. The monte carlo method. *Scientific American*, 192:90–96, 1955.
- [26] Paulo RS Mendonça and Roberto Cipolla. A simple technique for self-calibration. In *Computer Vision and Pattern Recognition, 1999. IEEE Computer Society Conference on.*, volume 1. IEEE, 1999.
- [27] J.M. Morel and G. Yu. Asift: A new framework for fully affine invariant image comparison. *SIAM Journal on Imaging Sciences*, 2(2):438–469, 2009.
- [28] R.A. Newcombe, S.J. Lovegrove, and A.J. Davison. Dtm: Dense tracking and mapping in real-time. In *Computer Vision (ICCV), 2011 IEEE International Conference on*, pages 2320–2327. IEEE, 2011.
- [29] Benjamin Ochoa and Serge Belongie. Covariance propagation for guided matching. In *Proceedings of the Workshop on Statistical Methods in Multi-Image and Video Processing (SMVP)*, 2006.
- [30] Alain Pagani, Christiano Gava, Yan Cui, Bernd Krolla, Jean-Marc Hengen, and Didier Stricker. Dense 3d point cloud generation from multiple high-resolution spherical images. In *12th International Symposium on Virtual Reality, Archaeology and Cultural Heritage (VAST)*, pages 17–24, 2011.
- [31] Alain Pagani and Didier Stricker. Structure from motion using full spherical panoramic cameras. In *Computer Vision Workshops (ICCV Workshops), 2011 IEEE International Conference on*, pages 375–382. IEEE, 2011.
- [32] Marc Pollefeys, Reinhard Koch, and Luc Van Gool. Self-calibration and metric reconstruction inspite of varying and unknown intrinsic camera parameters. *International Journal of Computer Vision*, 32(1):7–25, 1999.
- [33] T Schenk. Introduction to photogrammetry. *The Ohio State University, Columbus*, 2005.
- [34] Steven M Seitz, Brian Curless, James Diebel, Daniel Scharstein, and Richard Szeliski. A comparison and evaluation of multi-view stereo reconstruction algorithms. In *Computer Vision and Pattern Recognition, 2006 IEEE Computer Society Conference on*, volume 1, pages 519–528. IEEE, 2006.
- [35] Spheron vr sceneCam[®] HDR. <http://www.spheron.com/?id=107>.
- [36] C. Strecha, W. Von Hansen, L. Van Gool, P. Fua, and U. Thoennessen. On benchmarking camera calibration and multi-view stereo for high resolution imagery. 2008.
- [37] F. Sur. Robust matching in an uncertain world. In *2010 International Conference on Pattern Recognition*, pages 2350–2353. IEEE, 2010.
- [38] Frédéric SUR, N. NOURY, and M.O. BERGER. Computing the uncertainty of the 8 point algorithm for fundamental matrix estimation. 2008.
- [39] A. Torii, A. Imiya, and N. Ohnishi. Two-and three-view geometry for spherical cameras. In *Proc. Workshop Omnidirect. Vis*, pages 1–8. Citeseer, 2005.
- [40] George Vogiatzis and Carlos Hernández. Automatic camera pose estimation from dot pattern, <http://george-vogiatzis.org/calib/>, 2010.
- [41] Weiss ag civetta 360° camera. <http://www.weiss-ag.org/business-divisions/civetta/>.
- [42] Changchang Wu, Sameer Agarwal, Brian Curless, and Steven M Seitz. Multicore bundle adjustment. In *Computer Vision and Pattern Recognition (CVPR), 2011 IEEE Conference on*, pages 3057–3064. IEEE, 2011.
- [43] Christopher Zach. Simple sparse bundle adjustment, <http://www.inf.ethz.ch/personal/chzach/opensource.html>, 2011.
- [44] B. Zeisl, P. Georgel, F. Schweiger, E. Steinbach, and N. Navab. Estimation of location uncertainty for scale invariant feature points. *BMVC*, 2009.